New insights on the geochemical affinity and age of mineralized rocks in Timok magmatic complex, East Serbia

Miloš Velojić[1], Dina Klimentyeva[2], Albrecht von Quadt[3], Marcel Guillong[3], Frank Melcher[4], Thomas Meisel[4] & Dejan Prelević[1]

Key words:
Bor, Čukaru Peki,
Bor metallogenic zone,
porphyry, adakites, zircons.

Abstract. Bor and Čukaru Peki are world-class porphyry deposits spatially and genetically associated with the Cretaceous Timok magmatic complex. This research was conducted to determine the age and geochemical affinity of the magmatic rocks that formed these ore deposits. Our new geochemical analyses of magmatic rocks from Bor and Čukaru Peki deposits imply they comprise adakite-like compositions that have undergone the amphibole fractionation and sulphide saturation processes. The zircon ages indicate that the Bor system was formed in the age span between 84.5–82 Ma, while the Čukaru Peki system was created in the age span between 86.5–85 Ma.

Кључне речи:
Бор, Чукару Пеки,
борска металогенетска зона,
порфирска лежишта, адакити,
циркони.

Апстракт. Бор и Чукару Пеки су порфирска лежишта светских размера која су просторно и генетски везана са Тимочким магматским комплексом кредне старости. Ово истраживање је спроведено како би се утврдила старост и геохемијски афинитет магматских стена које су довеле до формирања ових лежишта. Наше геохемијске анализе указују да су и Бор и Чукару Пеки формирани из магматских стена које су сличне адакитима и које су током процеса формирања прошле кроз фазу фракционације амфибола и засићења сулфидима. Мерења старости циркона указују да је Борски систем настао у временском распону од 84.5–82 Ma, док је Чукару Пеки систем настао у временском периоду између 86.5–85 Ma.

[1] University of Belgrade, Faculty of Mining and Geology, Đušina 7, Belgrade, Serbia. E-mail: milos.velojic@rgf.bg.ac.rs

[2] GoldSpot Discoveries Corp., 64 Yonge Street, Suite 1010, Toronto, ON M5B 1S8, Canada.

[3] Department of Earth Sciences, ETH Zurich, 8092 Zurich, Switzerland.

[4] Montanuniversität Leoben, Franz Josef-Straße 18, 8700 Leoben, Austria.

Introduction

In the Balkan section of the Alpine-Hymalayan orogenic belt, several continental blocks were accreted to the Eurasian margin from Late Cretaceous to Eocene by decoupling crustal nappes from the subducting lithosphere (Menant et al., 2018). This accretion has resulted in the building of the orogenic belts, such as the Carpathian embayment and the Dinarides-Hellenides. The Apuseni–Banat–Timok–Srednogorie (ABTS) metallogenic and magmatic belt in this zone that stretches over 1500 km across Romania, Serbia, and Bulgaria probably reflects the final closure of that part of the Neotethys Ocean and the start of collision with the Adria/Europe block (Gallhofer et al., 2015). In Oligocene and Miocene, during the Laramian phase of Alpine orogenesis, this belt was deformed by oroclinal bending (Neubauer, 2002). The consequence of this bending is the shortening and elongation of the Serbian segment of the zone and its clockwise rotation by 30–70°, which resulted in its present lenticular shape and N–S orientation (Fügenschuh & Schmid, 2005; Knaak et al., 2016).

The Bor metallogenic zone represents a part of the ABTS belt; other well-endowed metallogenic areas host active mines of Chelopech and Elatzite in Bulgaria, Rosia Montana prospect in Romania, and Bor, Veliki Krivelj, Majdanpek, and Čukaru Peki in Serbia (Fig. 1) (e.g., Neubauer, 2002). The Timok magmatic complex is located in the Serbian part of the ABTS belt, with an area of 85x25 km (e.g., Janković, 1990).

This metallogenic belt is interpreted as being formed in an Andean-type scenario as a magmatic arc installed onto the European continent during the Late Cretaceous north-eastward subduction of the oceanic lithosphere of the alleged Sava Ocean (e.g., Neubauer, 2002; Fügenschuh & Schmid, 2005; Gallhofer et al., 2015; Menant et al., 2018). The gradual decrease in the age of magmatic rocks from east to west in the Serbian segment of the belt is explained by roll-back processes of the subducted lithosphere and the accretion of sediments in the forearc basin, which led to the gradual migration of the subduction zone (Kolb et al., 2013). This also implies that the Serbian segment of the arc was affected by
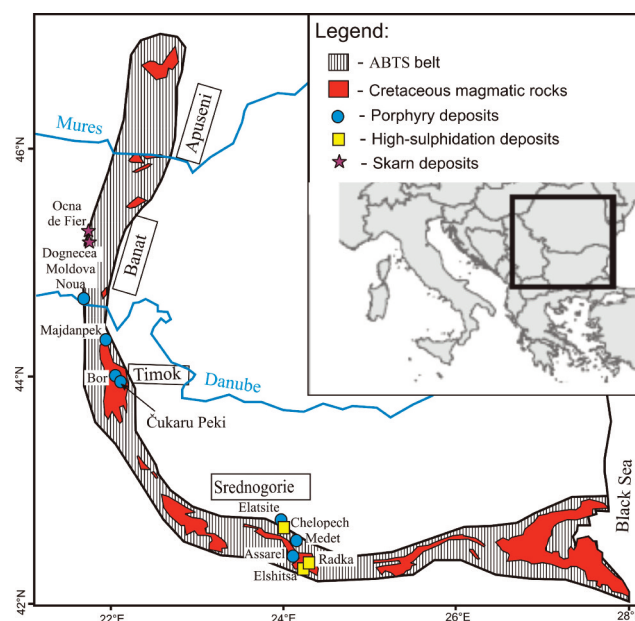

Fig. 1. Simplified map of the ABTS belt with metallogenic zones, magmatic intrusions, and major ore deposits (modified from Knaak et al. 2016).

extensional and transtensional tectonic regimes (Zimmerman et al., 2008; Knaak et al., 2016).

The Timok magmatic complex consists of three volcanic phases (Fig. 2.) (Gallhofer et al., 2015). Phase I andesites or "Timok andesites" contain coarse-grained euhedral amphibole phenocrysts and plagioclase in similar proportions, with a subordinate amount of quartz, biotite, and magnetite (Banješević, 2010; Banješević et al., 2019) and are exposed predominantly on the Eastern part of the Timok magmatic complex. It is generally accepted (Janković, 1990; Banješević, 2010; Kolb et al., 2013; Jelenković et al., 2016) that most of the ore deposits in the Bor metallogenic zone are genetically related to the first volcanic phase. The crystallization age of this phase's rocks was between 86.9 and 84.6 Ma (von Quadt et al., 2002). Phase II andesite is comprised of pyroxene and plagioclase with a subordinate amphibole (Banješević, 2010). The age of the rocks from the second phase was 82.35±0.352 Ma (von Quadt et al., 2002). Phase III concludes the volcanic activity in the Timok complex and is expressed in latite dykes and subvolcanic intrusions in the southwestern part of the complex. The age of these rocks is still poorly constrained (Banješević, 2010; Kolb et al., 2013).

Along with volcanic activity in this complex, intrusive magmatic rocks were emplaced as stocks and dykes. Most of the intrusive rocks in this complex were emplaced in shallow levels, occurring with varying relations of phenocrysts in the rock matrix due to the rapid cooling process (KOLB et al., 2013). The largest intrusive complex in Bor metallogenic zone is the Valja Strž intrusive complex (Fig. 2), which is composed of monzonites, diorites, quartz-diorites, syenites, and gabbros (BANJEŠEVIĆ, 2010) and its age was determined at 82.5–78.6 Ma (KOLB et al., 2013). Except for a porphyry Cu-Au system at Crna Reka and sediment-hosted Au deposits at Kraku Pešter and Bigar Hill, no other hydrothermal system can be genetically related to the Valja Strž monzonite, despite having several porphyry, polymetallic replacement, and sediment-hosted Au deposits in the vicinity (KNAAK et al., 2016).
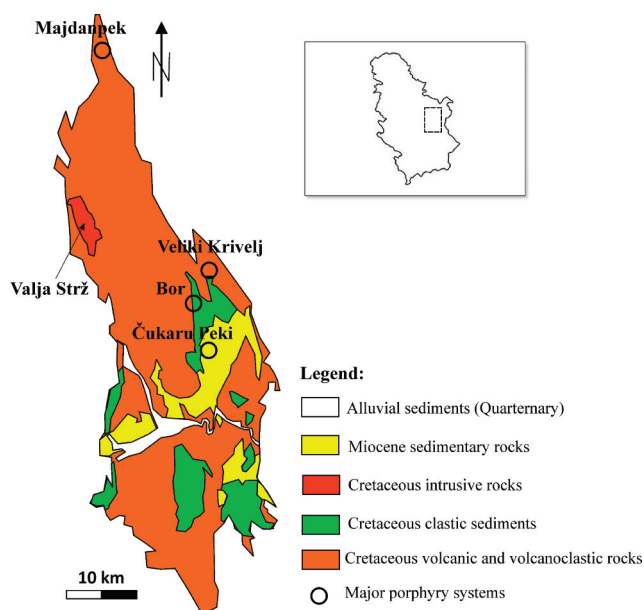
Fig. 2. *Simplified geological map of the Timok magmatic complex with marked locations of major porphyry deposits and Valja Strž intrusive complex (modified from JANKOVIĆ et al., 2002; KNAAK et al., 2016).*

STEIN et al. (2002) have conducted bulk rock measurements of rare earth elements of the Timok magmatic complex and concluded that these rocks have adakitic affinities since they have relatively high concentrations of Al_2O_3 and Sr, with low concentrations of Y and HREE (heavy rare earth elements). Considering these facts, they argued that the magmatic intrusive was probably formed by direct partial melting of the mafic protolith. KOLB et al. (2013) have argued that the rocks with adakitic affinity in the Timok magmatic complex were probably formed by high-pressure intense amphibole fractionation in lower crustal conditions. On the other hand, rocks with the affinity of normal-arc andesites were formed in upper crustal processes of combined fractionation and assimilation of crustal rocks.

So far, numerous authors have measured geochronological data of the Bor metallogenic zone by applying different methods (Table 1). JANKOVIĆ et al. (1981) have performed whole rock ages using the K-Ar and Rb-Sr method, resulting in K-Ar ages between 91 and 60 Ma and whole rock Rb-Sr ages between 108 and 55 Ma. VON QUADT et al. (2002) measured the ages of zircons from different phases of magmatism in the Timok magmatic complex and argued that the main mineralization activity lasted from 86 until 83 Ma. CLARK & ULLRICH (2004) have used the Ar-Ar method to obtain the age of mineralization in Majdanpek and concluded that it was formed at 84–83.6 ± 0.6 Ma. LIPS et al. (2004) argued that the average age of igneous hornblende in Bor, measured by the Ar-Ar method is between 84.6 and 83.4 Ma. LEROUGE et al. (2005) have performed K-Ar measurements on alteration alunite from Bor and calculated an age of 84.6 ± 1.2 Ma. Re-Os dating on molybdenite revealed ages of 86.24 ± 0.4 and 85.94 ± 0.4 Ma for Bor and 87.88 ± 0.5 Ma for Veliki Krivelj (ZIMMERMAN et al., 2008). KOLB et al. (2013) dated zircons from the Timok andesite complex and argued that the volcanic rocks in the eastern part of the complex (89.9–82.8 Ma) are older than volcanic rocks in the western part (82.2–78.9Ma). KNAAK et al. (2016) performed SHRIMP U-Pb dating of different intrusives near the Valja Strž intrusive complex and calculated ages between 83.6–78.5 Ma. BANJEŠEVIĆ et al. (2019) have analyzed volcanic rocks near Čukaru Peki and argued that there are two magmatic phases: the first phase (V1A) – older andesites with adakitic affinity show an age of 90.1 Ma and the second phase (V1B)- younger non-mineralized andesites with an age of 85.2 Ma (Table 1).

Table 1. Summary of the geochronological data of the magmatic minerals from the Timok magmatic complex.

Source	Method	Age
Janković et al. (1981)	K-Ar whole rock	91–60 Ma
Janković et al. (1981)	Rb-Sr whole rock	108–55 Ma
Von Quadt et al. (2002)	U-Pb zircon	86.6–83.1 Ma
Clark & Ullrich (2004)	Ar-Ar mineral	Biotite: 89.0–83.6 Ma
Lips et al. (2004)	Ar-Ar mineral	Hornblende: 85–83 Ma
		84.6–83.4 Ma
Kolb et al. (2013)	U-Pb zircon	Eastern part of TMC: 89.9–82.8 Ma
		Western part of TMC: 82.2–78.9 Ma
		Bor: 86.3–86.2Ma
		Veliki Krivelj: 84.7Ma
Knaak et al. (2016)	U-Pb zircon SHRIMP	Valja Strž 82.5–78.5 Ma
		Čoka Kuruga 83.6 Ma
		Dumitru Potok 82.1–81.6Ma
		Kraku Riđi 80.8 Ma
Banješević et al. (2019)	U-Pb zircon	V1A 90.1 Ma
		V1B 85.2 Ma

In this study, we have two distinct aims:

1) A better understanding of the geochemical process that led to the formation of ore deposits in this magmatic complex

2) Better constraining of the ages of mineralization of the largest porphyry deposits in this complex: Bor and Čukaru Peki

To find the answers to these questions, we have sampled rocks from Bor and Čukaru Peki and performed bulk-rock analysis and LA-ICP-MS analysis on zircons, which will be presented in this paper.

Geology of the Bor deposit

The Bor deposit is hosted by Phase I andesites (Fig. 3) and is truncated by the reverse Bor fault that dips approximately 75° SSE, with barren Bor conglomerates outcropping to the East of the fault (Janković et al., 2002; Đorđević, 2005; Klimentyeva et al., 2022). Phase I andesites are unconformably overlain by a package of marls approximately 150 m thick. Host rock andesites are hornblende-phyric, with euhedral hornblende, plagioclase and subordinate euhedral to subhedral biotite.

The host rock andesite is altered to chlorite-sericite with associated magnetite-chalcopyrite-

quartz vein mineralization in the deep Borska Reka porphyry. Toward the shallow part of the Borska Reka porphyry, the alteration style changes to texture-destructive sericite-kaolinite alteration, which is overlain by anhydrite-kaolinite alteration zone with anhydrite-sulfide veins, referred to as Tilva Ros epithermal mineralization zone and surrounded by the massive sulfide lens-like orebodies, including recently mined out T, T1 and historic Tilva Mika, Čoka Dulkan, E, E 1 and others (Jelenković et al., 2001; Janković et al., 2002; Koželj, 2002). The massive sulfide lenses are approximately 50x50x70 meters and are composed of chalcocite, covellite, and pyrite with some residual quartz; one mined-out massive sulfide orebody, L, was composed of solid sulfur and massive sulfide in approximately 70/30 proportion (Janković et al., 2002).

Geology of the Čukaru Peki deposit

Čukaru Peki is a recently discovered porphyry-epithermal ore deposit located only 5 km south of Bor (Jelenković, 2014). The mineralization at the Čukaru Peki can be genetically classified as a high-sulphidation epithermal and porphyry copper-gold deposit (Banješević & Large, 2014). It occurs at depths between 400 and more than 2000 m below the surface (Fig. 3).

The host rocks are Upper Cretaceous Phase 1 volcanics (Lower andesites), including andesites, andesite breccias, hydrothermal breccia, and diorites in deeper parts. Small clay-rich fault breccias are also relatively common throughout the volcanics. Immediately overlying the host andesite volcanics is a relatively unaltered andesitic unit that varies in thickness from a few meters up to approximately 50 m (Upper andesites). Overlying the

Upper andesite is a Late Cretaceous sequence of marl, sandstones, and conglomerates which dips at a shallow angle to the west. This Late Cretaceous sequence is unconformably overlain by Miocene conglomerates and sandstones, which dip at a low angle to the east and which vary from 200 to 400 m in thickness within the Čukaru Peki deposit area (Jakubec et al., 2018; Banješević et al., 2019).

Banješević et al. (2019) use the terms V1A and V1B for Lower and Upper andesites, respectively. V1A andesite is plagioclase-rich, holocrystalline, and hydrothermally altered, while on the other hand, V1B is hornblende-rich, holo- to hypo-crystalline non-mineralized andesite.

separation was based on the textural features of the rocks and the presence of different veins and alterations. The types of diorites are the following:

1) P1 - Diorite with indistinguishable texture, which is intensely altered by silicification (Fig. 4a). Commonly contains quartz veins and orange anhydrite veins.

2) P2 - Diorite with visible phaneritic texture; common alterations are potassic and chloritic. It also contains many quartz veins (Fig. 4b).

3) P4 - Diorite with porphyritic texture, similar to andesite, due to the presence of plagioclase phenocrysts. Contains anhydrite and gypsum veins, with a smaller amount of quartz veins.
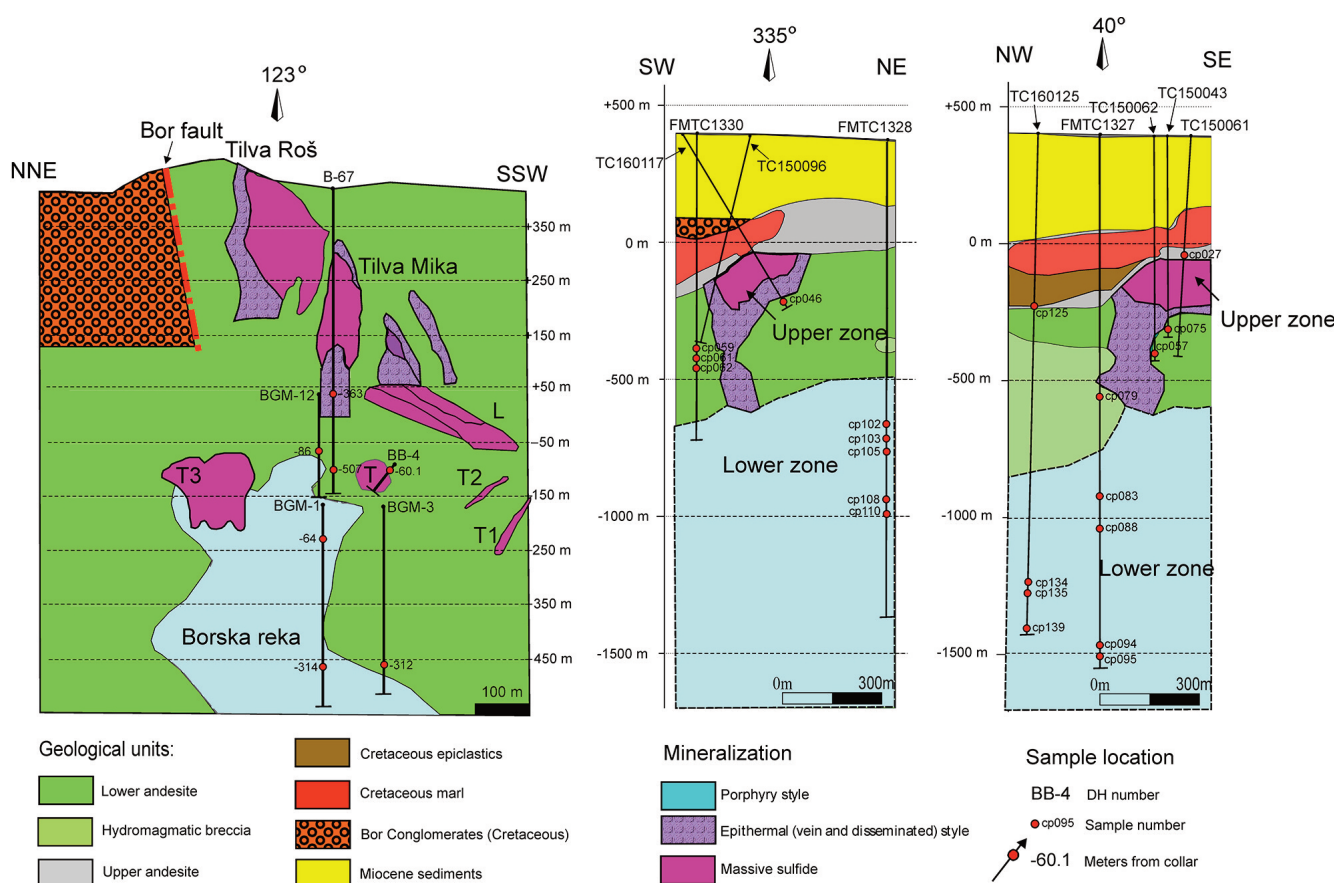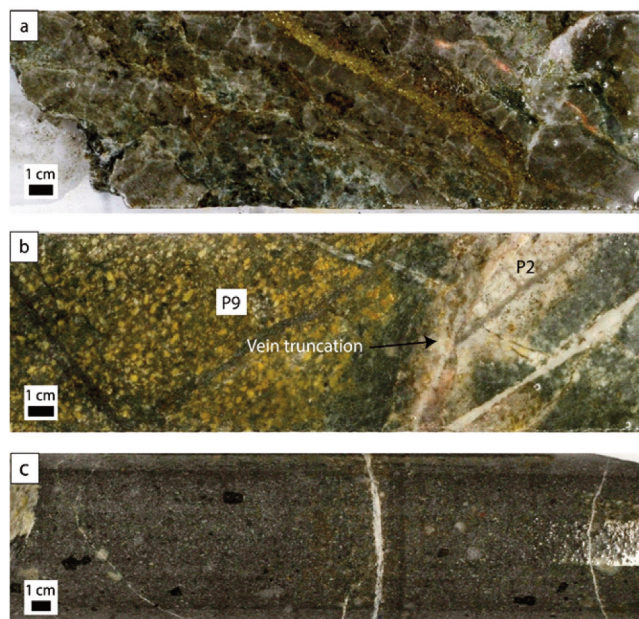

Fig. 3. *Cross-section of Bor and two cross-sections of Čukaru Peki deposits with locations of samples for bulk-rock analysis and U-Pb geochronology (red circle marks). Modified after Starostin (1970); Janković et al. (2002); Jelenković et al. (2016), with additions based on Bor and Čukaru Peki geologic documentation. Čukaru Peki sections were modelled in Leapfrog software based on the logging of the presented drill holes.*

Several types of diorite dykes were distinguished by geologists of Rakita Exploration company in the Lower zone (porphyry part of Čukaru Peki). The

4) P9 - Diorite with yellowish colour and distinct phaneritic texture but fewer veins. The most common alteration is chloritization (Fig. 4b).

Miloš Velojić, Dina Klimentyeva, Albrecht von Quadt, Marcel Guillong, Frank Melcher, Thomas Meisel & Dejan Prelević

5) P10 - Late grey unaltered diorite dykes which don't contain any veins (Fig. 4c).

Fig. 4. Illustration of different porphyry intrusions from Čukaru Peki. a) Very altered P1 diorite from TC160125 drill hole; b) Contact between P2 and P9 porphyries with an arrow pointing at a vein truncation in P2 dyke from FMTC1328 drill hole; c) Unaltered and unmineralized P10 diorite from TC160125 drillhole.

Jelenković et al. (2016) describe three types of mineralization at Čukaru Peki: 1) Porphyry type - in deeper parts of the Čukaru Peki deposit, at depths more significant than 1000 m from the surface. Anhydrite and quartz veins are commonly associated with this type of mineralization. 2) Transitional epithermal zone between the high sulphidation and porphyry Cu-Au mineralization zones. It comprises covellite and enargite replacing the primary sulphide (chalcopyrite) in porphyry Cu-Au mineralization and is associated with gypsum, anhydrite, and calcite veins. Locally-developed argillic alteration (dominated by kaolinite and/or montmorillonite) variably overprints high-sulphidation and porphyry-style alteration. 3) High sulphidation type- with Cu-Au massive-sulphides, veins with pyrite and covellite, and hydrothermal breccias. This type of mineralization forms a single zone, well defined by intense alteration and pyritization at depths ranging from 400 to over 1000 m below the surface. The predominant sulphides are covellite with pyrite, enargite, and chalcocite. Dominant alteration assemblage in this zone is typically advanced argillic.

Samples

Preserved core from geotechnical drill holes and samples from the massive sulfide T orebody of the locality Bor are used as a basis for this study.

Due to intensive alteration overprint and the lack of well-defined magmatic contacts, vein truncations, and alignment of phenocrysts along the contacts, we selected samples for dating and geochemical analysis from the different levels of the deposit. Phase I andesite, weakly altered and barren, overlies the Borska reka porphyry and Tilva Roš epithermal orebodies and represents the host rock (sample B67-363, Fig. 5a). Silicified diorite dyke with the anhydrite-kaolinite alteration from the shallow level of the deposit represents syn-to post-mineral phase, with small-scale dissemination of covellite. Samples from the deep porphyry zone of Borska Reka (BGM3-312 and BGM1-314, Figs. 5c and 5d) are heavily altered and mineralized. They could represent the more intensively altered variant of the overlying andesite volcanics, with a decreased modal abundance of plagioclase due to its alteration to sericite and kaolinite. They, therefore, could be correlated to V1A and V1B
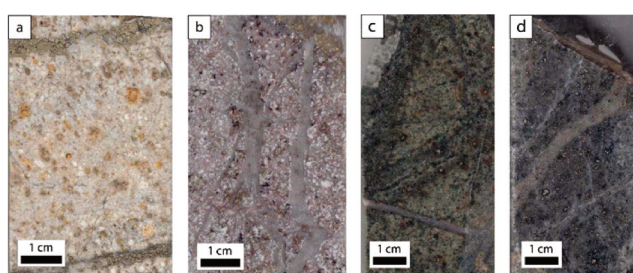
Fig. 5. Bor samples selected for zircon geochronology. a) Altered Phase I andesite overlying Borska Reka and Tilva Roš deposits, with pyrite-anhydrite veins; B67-373; b) Fine-grained diorite dyke from shallow levels of Borska Reka porphyry, with sinuous quartz veins, disseminated covellite; BGM1-64.8; c) Deep, heavily altered Phase I andesite from Borska Reka porphyry, with quartz-pyrite-chalcopyrite veins and pyrite-anhydrite veinlets with chlorite-sericite halos; BGM3-312; d) Deep Borska Reka porphyry with prominent chalcopyrite-pyrite disseminations and hairline pyrite stringers; BGM1-314.

in andesite phases from Čukaru Peki (Banješević et al., 2019).

Around 140 samples were sampled from 9 drill holes from Čukaru Peki: FMTC1327, FMTC1328, FMTC1330, TC140053, and TC150061. TC150062, TC150096, TC160117 and TC160125. These drill holes were picked because they contain significant intersections with high-sulphidation mineralization (TC140053, TC150061. TC150062, TC150096, TC160117) and porhyry-style mineralization (FMTC1327, FMTC1328, and TC160125). FMTC1330 was picked for sampling because it is a part of the same cross-section as several other drillholes, but it was drilled at the outer edge of the high-sulphidation system.

Most of the Lower andesite samples are altered by advanced argillic or argillic alteration and mineralized to a certain extent, whereas upper andesite samples are unaltered and barren. Most Upper diorite samples from the porphyry zone of Čukaru Peki are altered and mineralized. The only exception is three samples of P10 porphyry dykes, which were taken just for dating purposes.

Twenty-one rock samples from Čukaru Peki and three from Bor were selected for bulk rock chemistry. We have chosen siginifanctly more samples from Čukaru Peki to analyze different types of andesites and diorite dykes. Also, bulk rock analysis of rocks from Bor is already known from previous research (e.g., Kolb et al., 2013). Four samples from Čukaru Peki porphyry intrusions and five samples from Bor were selected for zircon dating and trace element measurements. The selection of samples for geochronology was based on their textural differences and the presence of alterations (see Fig. 4 and Fig. 5). Selected samples for this study are shown in Table 2.

Methods

XRF glass beads were prepared of all Bor samples (major and trace elements). Core samples were cleaned and crushed in a hydraulic press, with approximately 50–70 grams of rock chips from each sample subsequently crushed in an agate mill. A 0.5-gram aliquot of sample powder was mixed with 1.5

grams of $LiNO_3$ and 6.6 grams of $Li_2O_4B_7$, and the mixture was first gradually heated from 300 °C to 800 °C for 1 hour to allow for complete oxidation of sulfide minerals with the nitrate to lithium sulfate. The mixture was molten at 1000 °C. Quenched glass beads were analyzed for major elements (Si, Ti, Al, Fe, Mn, Mg, Ca, Na, K, P, S, Cu) by X-ray fluorescence (XRF) using an Axios PANalytical WD-XRF spectrometer at ETH Zürich and quantified with 34 standard reference materials. Klimentyeva et al. (2021) describe the method used and the analytical precision. Laser Ablation determined trace elements – Inductively Coupled Plasma – Mass Spectrometry (LA-ICP-MS) at ETH Zürich (Switzerland) on shards of broken glass beads, using at least three ablation spots of 115 μm diameter, a repetition rate of 10 Hz, and a laser energy density of 8–10 J·cm^{-2}. NIST 610 glass reference material served as an external calibration standard, and the TiO_2 content of the sample obtained by XRF was used as an internal standard for the LA-ICP-MS traces. LA-ICP-MS intensities were processed using the MatLab-based SILLS software (Guillong et al., 2008). Previous research (e.g., Günther et al., 2001; Ling et al., 2014) has demonstrated that combining XRF and LA-ICP-MS provides accurate bulk rock element concentrations comparable to standard ICP-MS analysis.

Samples from Čukaru Peki were digested using the sodium peroxide digestion method at Montanuniversitat Leoben, Austria (Bokhari & Meisel, 2016). GBW07104 andesite standard was used as an external standard. For internal standard, 0,1 ml of 1 mg l-1 Ge, In, and Re was added each to 5 ml of a 1:5 test solution. An Agilent 7500cx ICPMS instrument (at Montanuniversitat Leoben, Austria) was used for sample analysis. The analytical precision of the digestion method and the instrument is described in Bokhari & Meisel (2016). REE and trace element concentrations were normalized to C1-chondrite, and multielement concentrations were normalized to the primitive mantle.

Samples for geochronology were disintegrated using a Selfrag device at ETH Zurich, processed with panning and magnetic separation, and hand-picked under a binocular lens for zircons. The selected 20–50 zircon grains were then annealed for 48 hours in the oven at 900 °C before polishing and measuring.

Geol. an. Balk. poluos., 2023, 84 (1), 47–63

53

Table 2. Analyzed samples from Čukaru Peki and Bor including drill hole number and lithological description.

Samples used for bulk-rock analysis, Čukaru Peki		
Sample number	Drillhole number	Lithology
Cp027	TC150061	Unaltered upper andesite with calcite vein
Cp046	TC160117	Lower andesite containing late gypsum vein and native sulphur
Cp057	TC150062	Lower andesite containing anhydrite vein with pyrite
Cp059	FMTC1330	Lower andesite with gypsum vein
Cp061	FMTC1330	Oxidized lower andesite with quartz-calcite vein
Cp062	FMTC1330	Lower andesite with calcite-zeolite vein
Cp075	TC140053	Lower andesite with pyrite-covellite vein
Cp079	FMTC1327	Lower andesite with pyrite-enargite vein and pink alunite
Cp083	FMTC1327	Unaltered P10 porphyry
Cp088	FMTC1327	Lower andesite altered by chloritization
Cp094	FMTC1327	P4 porphyry with thin quartz vein
Cp095	FMTC1327	P2 porphyry with thick mineralized quartz veins (probably B veins)
Cp102	FMTC1328	Unaltered P10 porphyry
Cp103	FMTC1328	P2 porphyry with quartz veins
Cp105	FMTC1328	P2 porphyry with mineralized quartz veins (probably B veins)
Cp108	FMTC1328	P9 porphyry with purple anhydrite vein
Cp110	FMTC1328	P2 porphyry with thick purple anhydrite vein
Cp125	TC160125	Unaltered upper andesite with calcite vein
Cp134	TC160125	Unaltered P10 porphyry
Cp135	TC160125	P1 porphyry with pyrite vein (probably D vein)
Cp139	Tc160125	P1 porphyry with quartz vein (probably B vein)
Samples used for bulk-rock analysis, Bor		
BGM12-86	BGM12	Edge of the Tilva Roš high-sulfidation epithermal deposit
B67-258	B67	Weakly-altered andesite overlying Borska Reka porphyry
BB4-60.4	Bb4	Edge of the massive sulfide T orebody
Samples used for geochronology, Čukaru Peki		
Cp083	FMTC1327	Unaltered P10 porphyry
Cp095	FMTC1327	P2 porphyry with thick quartz veins (A or B veins)
Cp134	TC160125	Unaltered P10 porphyry
Cp135	Tc160125	P1 porphyry with pyrite vein (probably D vein)
Samples used for geochronology, Bor		
B67-363	B67	Weakly-altered andesite overlying Borska Reka porphyry
B67-507	B67	Andesite overlying Borska Reka porphyry, kaolinite-anhydrite alteration
BGM1-64.8	BGM-1	Late, low-grade porphyry dyke
BGM3-312	BGM-3	Deep Borska Reka porphyry
BGM1-314	BGM-1	Deep Borska Reka porphyry

To reveal the internal texture of the zircons and check for the presence of inherited cores, epoxy mounts were carbon-coated and investigated on the JEOL JSM-6390 LA scanning electron microscope (SEM) equipped with a Deben Centaurus panchromatic cathodoluminescence detector.

U-Pb ages of zircons were obtained by Laser Ablation – Inductively Coupled Plasma – Mass Spectrometry (LA-ICP-MS) at ETH Zürich, with 193-nm Resolution (S155) ArF excimer laser coupled to an Element XR sector-field ICP-MS; 30 μm spots were placed in the inclusion-free interior of the grains. 5 Hz

54

Geol. an. Balk. poluos., 2023, 84 (1), 47–63

repetition rate was used, and the blank signal of 20 seconds was followed by the ablation signal of 30 seconds; on-sample fluence was around 2.5–3.5 J/cm^2. LA-ICP-MS intensities were processed using Iolite software to obtain the ages and trace element contents. The following standards were measured after every set of 20 sample points: GJ-1 (JACKSON et al., 2004), 91500 (WIEDENBECK et al., 1995), AUSZ7-1 (KENNEDY et al., 2014) and Plešovice (SLÁMA et al., 2008) for ages and NIST-612 glass standard for trace elements; zircon blank was ablated together with the standards.

ICP-MS signals were processed with Iolite software (PATON et al., 2011), and the IsoplotR tool was used for plotting average ages (VERMEESCH, 2018). Samples that indicated Pb loss were excluded from the calculation.

Results

Geochemistry

REE patterns and multielement plots are presented in Fig.6. All data exhibit E-MORB patterns, which is a typical pattern for subduction zone magmas (SUN & MCDONOUGH, 1989). The general features of the analyzed samples are the enrichment in light REE (LREE) and relatively flat heavy REE (HREE) patterns, except for three samples from Čukaru Peki, which exhibit a significant depletion of HREE elements. According to some authors (e.g., DEFANT & DRUMMOND, 1990), this HREE depletion can indicate slab melting, while other authors (RICHARDS & KERRICH, 2007) associate this phenomenon with upper-crustal fractionation processes.

In multi-element plots (SUN & MCDONOUGH, 1989) (Fig. 6b), the analyzed samples show enrichment in large-ion lithophile elements (LILEs), such as Ba, Rb, Sr, U and Th, and depletion of Nb, Ta, and other high field strength elements (HFSEs, e.g., Zr and Hf).

Diagrams 7a and 7b show that some samples contain much higher Sr/Y and La/Yb ratios and plot in the adakite field, whereas most of the other samples plot in the normal arc field. On Dy/Yb vs. SiO$_2$ diagram (Fig.7c), most of the analyzed samples contain similar Dy/Yb ratios, with a slight decline in samples with higher amounts of SiO$_2$.
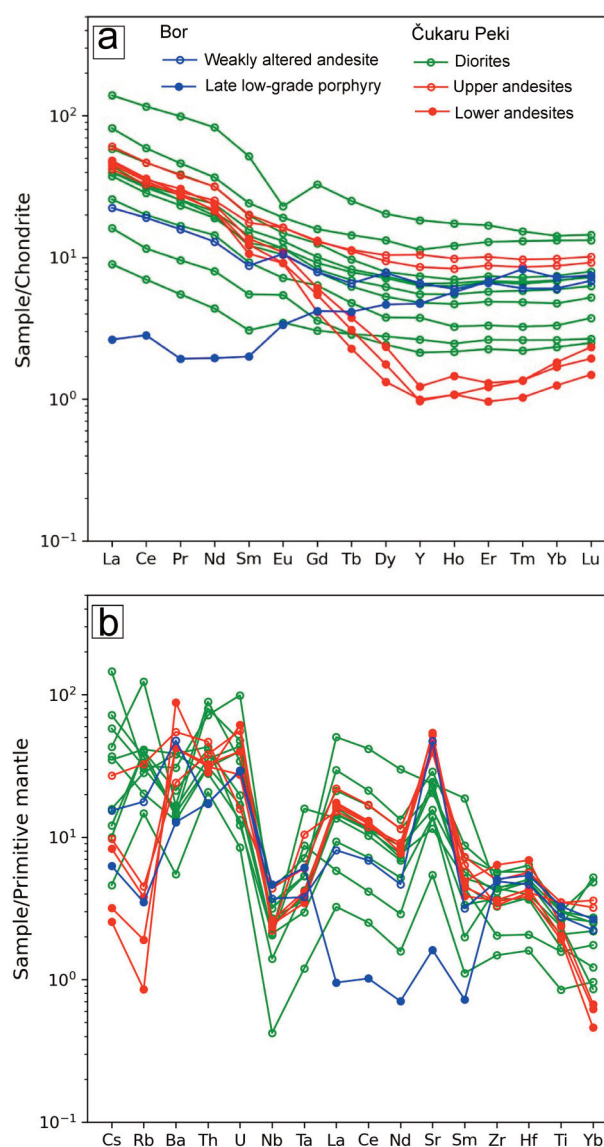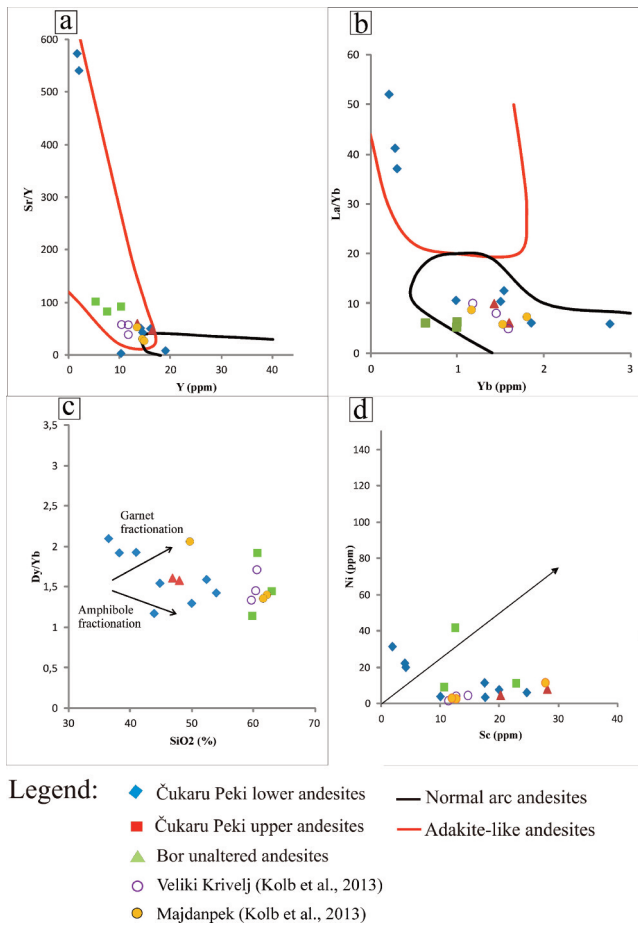

*Fig. 6. Trace element content of host rocks and porphyries from Bor and Čukaru Peki. **a)** REE, normalized to C1 chondrite (SUN & MCDONOUGH, 1989); **b)** Multielement plot, normalized to the primitive mantle.*

On Ni vs. Sc diagram (Fig. 7d), proposed by HALLEY (2020), most of the analyzed samples from Bor and Čukaru Peki show reduced concentrations of Ni compared to the correlation line with Sc (with a ratio of 1.5 to 1).

Geochronology results

U/Pb zircon ratios of samples from Čukaru Peki and Bor are available in Table 3, and the data are

Legend:
- ◆ Čukaru Peki lower andesites
- ■ Čukaru Peki upper andesites
- ▲ Bor unaltered andesites
- ○ Veliki Krivelj (Kolb et al., 2013)
- ● Majdanpek (Kolb et al., 2013)
- — Normal arc andesites
- — Adakite-like andesites

Fig. 7. Bulk-rock trace elements data from Bor and Čukaru Peki compared to data from Veliki Krivelj and Majdanpek, described in Kolb et al. (2013). **a)** *Data plotted on Sr/Y vs. Y diagram (adakite and normal arc field values from Richards & Kerrich, 2007);* **b)** *Data plotted on La/Yb vs. Yb diagram (adakite and normal arc field values from Richards & Kerrich, 2007);* **c)** *Data plotted on Dy/Yb vs. SiO$_2$ diagram with mineral fractionation paths from Davidson et al. (2007);* **d)** *Data plotted on Ni vs. Sc diagram with correlation line for Ni vs. Sc diagram from Halley (2020).*

plotted on concordia diagrams (Figs. 8, 9); the results of weighted mean $^{206}Pb/^{238}U$ average ages are shown in Fig. 10. The uncertainties calculated by internal procedures of Isoplot, as well as the areas of the Concordia ellipses, are far too small and do not reflect the actual uncertainties inherent to the LA-ICP-MS method, which is estimated to be between 1 and 3% of the calculated age (Chiaraida et al., 2013). Therefore realistic uncertainties were calculated and presented on the weighted mean average dia-

gram as 1.5% of the calculated age (von Quadt et al., 2014; Klimentyeva, 2022).

Zircons from Bor were divided into four groups based on the different rock-textures (see Fig. 5) and spatial distribution of the rocks in the hydrothermal system. The four groups are as follows: zircons from deep porphyry diorites of Borska Reka, zircons from late low-grade porphyries, zircons from heavily altered host rock andesites, and zircons from weakly altered andesites. Zircons from deep porphyry diorites cover a wide range of ages, between 84.5±1.27 Ma and 82.08±1.23 Ma. Zircons from late low-grade porphyries yield ages around 83.25±1.25 Ma. On the other hand, the age difference between host andesite groups is larger: heavily altered andesites have concordia age of 85.59±1.28 Ma, while the weakly altered andesites have concordia ages of 84.78±1.27 Ma.

Čukaru Peki zircons were divided into three groups: zircons from early porphyry diorites P1, zircon from mineralized P2 porphyries, and zircons from late non-mineralized dykes (P10 porphyries). The early diorite zircon group P1 has only three concordant zircons which don't overlap, with the ages of 95.7, 89.5, and 85.6 Ma. Mineralized P2 porphyries have concordia ages of 86.5±1.3 Ma, while the zircons from P10 late porphyries have concordia ages of around 85.03±1.28Ma.

Discussion

### The geochemical affinity of rocks

The plots of La/Yb versus Yb and Sr/Y versus Y (Figs. 7a, b) are generally used for distinguishing normal-arc magmas from adakite-like signatures, which are defined by La/Yb and Sr/Y ratios higher than 20 and Yb and Y contents below 1.9 and 18 ppm, respectively (Defant & Drummond, 1990; Richards & Kerrich, 2007). Due to their high Sr content, most of the samples from Bor and Čukaru Peki show adakite-like signatures on the Sr/Y versus Y diagram. On the other hand, apart from 3 samples from Čukaru Peki, most of the analyzed samples show normal arc signatures on La/Yb versus Yb diagram.

56

Geol. an. Balk. poluos., 2023, 84 (1), 47–63

Table 3. *U-Pb ICP-MS ages of Bor and Čukaru Peki samples. Realistic uncertainties were calculated as 1.5% of the calculated age. Age average is calculated by Isoplot software as weighted mean average of measured ages.*

Sample	Mean ratio Pb^{207}/U^{235}	Concordia age, Ma	2 sigma error, Ma	Uncertainty calculated by IsoplotR, Ma	Realistic uncertainty, Ma	Age average, Ma	Uncertainty calculated by Isoplot, Ma	Realistic uncertainty, Ma
Čukaru Peki								
P1 mineralized porphyry	0,096	N/A	1.1	0.32	1.33	88.25	0.28	1.3
P2 mineralized porphyry	0,090	86.5	1	0.13	1.30	86.5	0.13	1.3
P10 late non-mineralized porphyry	0,089	85.03	1.2	0.09	1.28	85.09	0.09	1.3
Bor								
B67-507 (heavily altered host rock andesite)	0,092	85.59	2.2	0.11	1.28	85.6	0.11	1.3
B67-363 (weakly altered host rock andesite)	0,091	84.78	2.1	0.15	1.27	84.79	0.15	1.3
BGM1-64.8 (low-grade post-mineral porphyry)	0,088	83.25	1.2	0.08	1.25	83.25	0.08	1.2
BGM3-312 (deep Borska Reka)	0,089	84.51	1.1	0.08	1.27	84.51	0.08	1.3
BGM1-314 (deep Borska Reka)	0,088	82.08	1.1	0.09	1.23	82.08	0.09	1.2
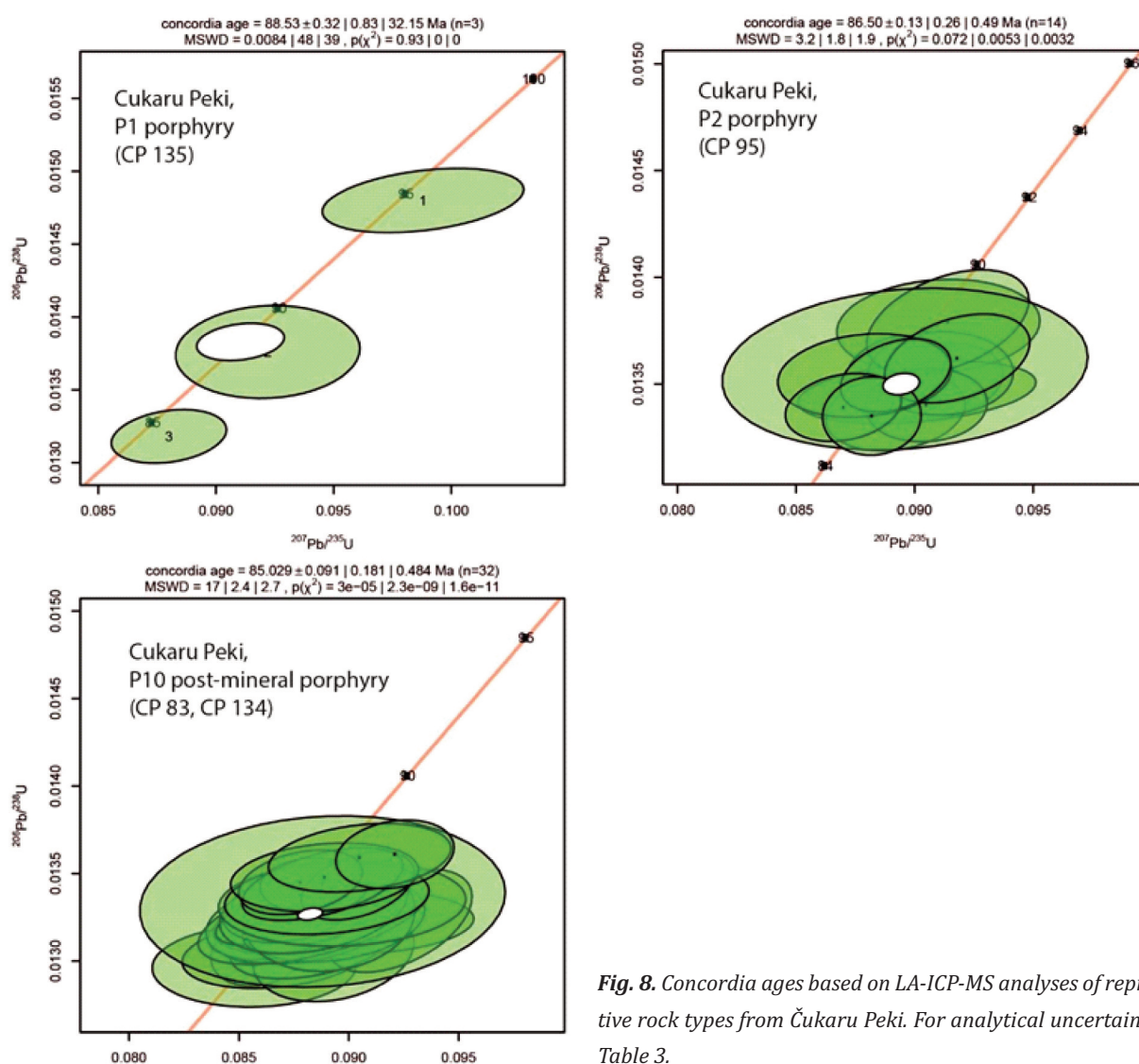
Fig. 8. *Concordia ages based on LA-ICP-MS analyses of representative rock types from Čukaru Peki. For analytical uncertainties, see Table 3.*

Geol. an. Balk. poluos., 2023, 84 (1), 47–63

57
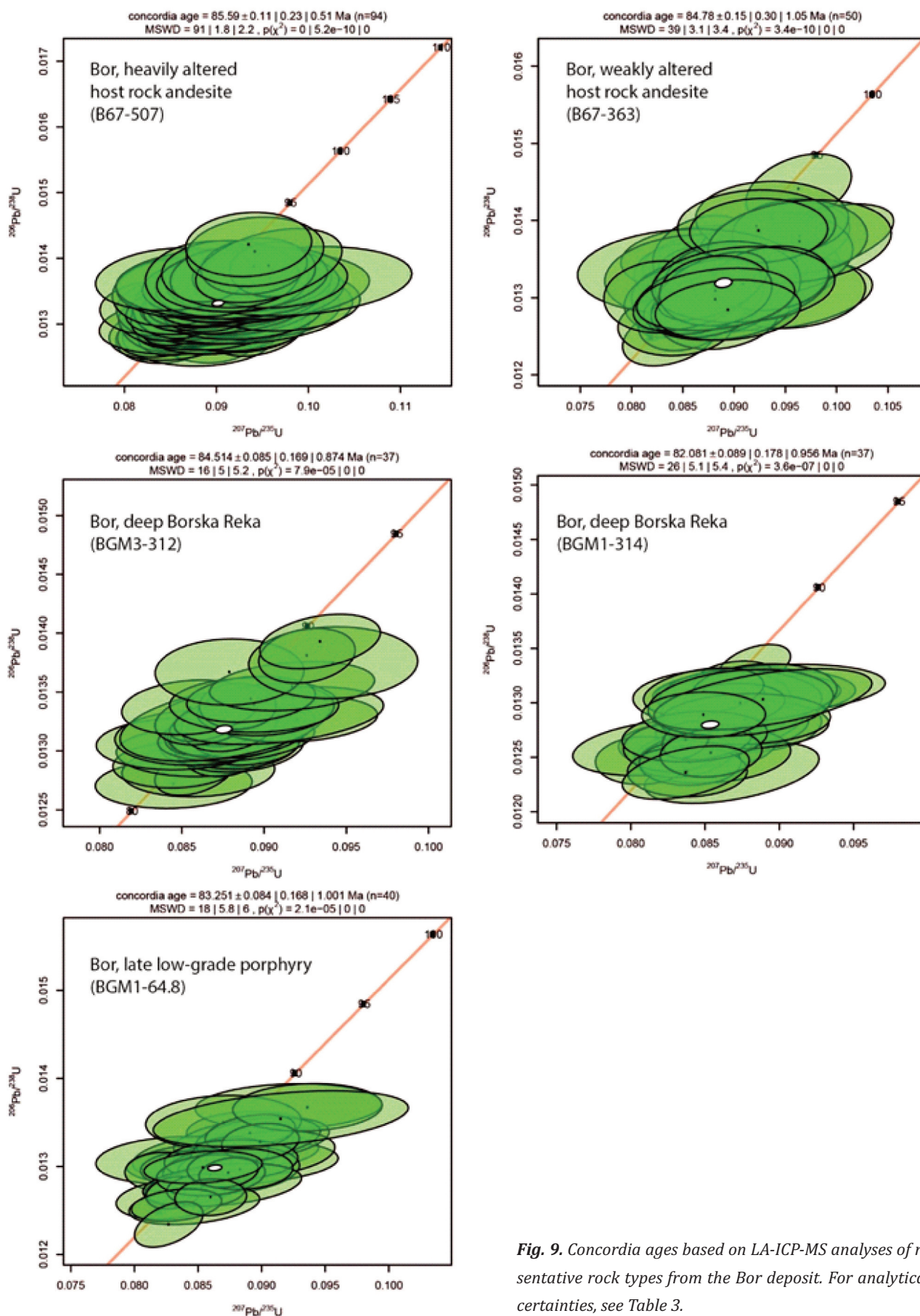
Fig. 9. *Concordia ages based on LA-ICP-MS analyses of representative rock types from the Bor deposit. For analytical uncertainties, see Table 3.*
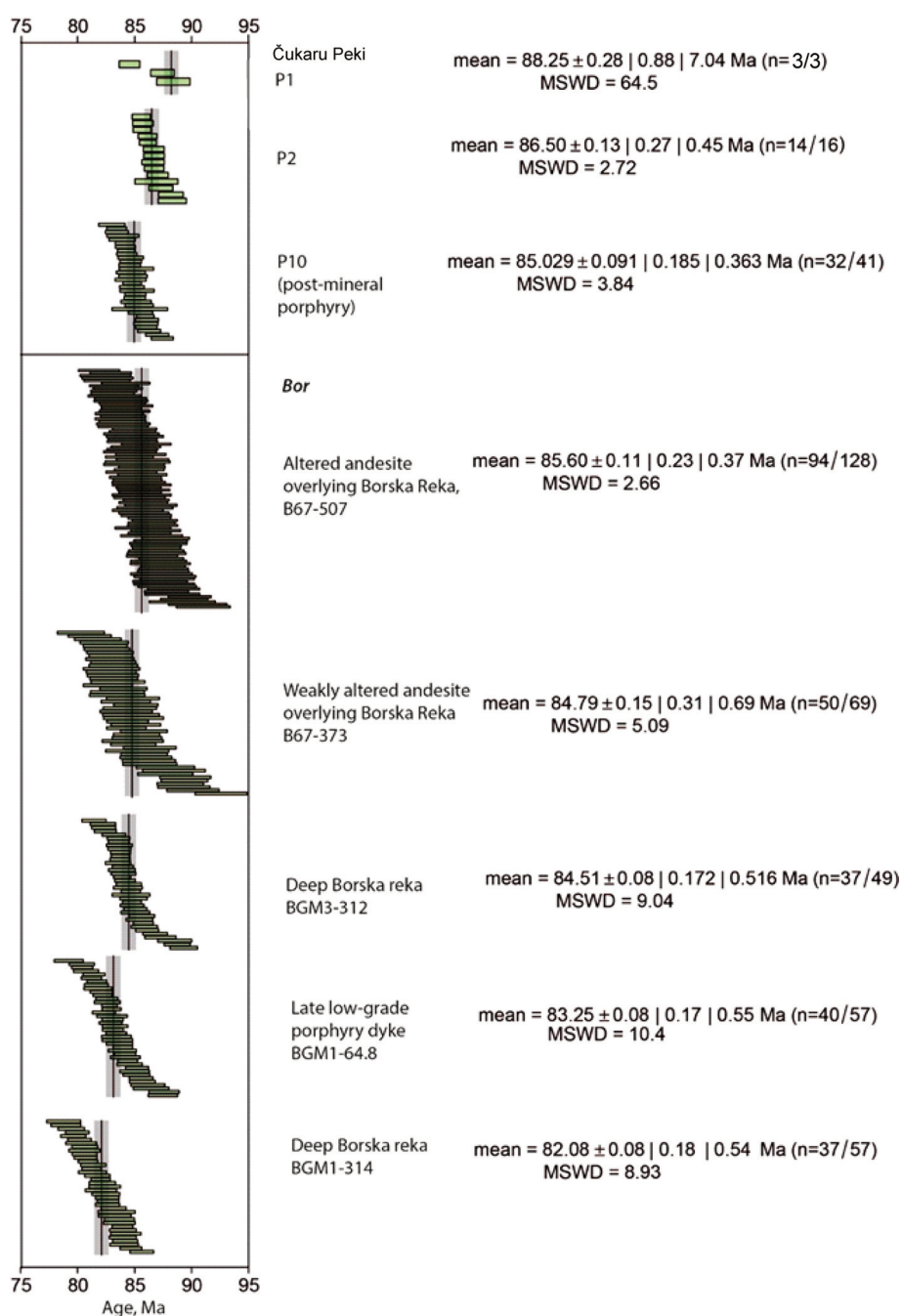
58

Geol. an. Balk. poluos., 2023, 84 (1), 47–63

Fig. 10. *Weighted average ages for representative rock samples from Bor and Čukaru Pek.*

Al_2O_3, <3 wt. % MgO, ≥400 ppm Sr, ≤18 ppm Y, ≤1.9 ppm Yb, ≥20 ppm Ni, ≥30 ppm Cr, Sr/Y ≥20 and La/Yb ≥20.) One of the most distinguishing features of these rocks is the depletion of middle REE (MREE) and heavy REE (HREE). Several authors interpret this depletion as an indicator of high-pressure fractionation of amphibole since this mineral commonly incorporates MREE and HREE (Castillo et al., 1999; Davidson et al., 2007). Kolb et al. (2013) argue that there is substantial evidence that the source of the Timok Magmatic Complex underwent high-pressure amphibole fractionation rather than garnet fractionation (which implies the presence of metasomatized mantle).

The Dy/Yb ratio versus SiO_2 diagram (Fig. 7c) may provide insight into mineral fractionation in the magma (Davidson et al., 2007). The analyzed samples have a general trend of a decrease in the Dy/Yb ratio with increasing SiO_2 concentrations, which implies amphibole rather than garnet fractionation.

In this study, we also use the Ni vs. Sc diagram recently proposed by Halley (2020) to distinguish igneous complexes which have undergone sulfide saturation. According to this publication, igneous rocks which do not contain olivine or clinopyroxene have a distinct correlation of Ni and Sc concentrations with a ratio of around 1.5 to 1. In melts that have undergone sulfide saturation, a mono-sulfide solid solution crystallizes with significant amounts of Ni and Co, which leaves the remaining silicate melt depleted in these

These samples are the same three samples that contain low HREE concentrations (Fig. 6a).

Similar to the previous bulk rock measurements of rocks from the Timok magmatic complex (Kolb et al., 2013; Gallhofer et al., 2015), some selected samples exhibit adakitic affinities. Richards & Kerrich (2007) define adakite-like rocks by the following composition: ≥ 56 wt. % SiO_2, ≥15 wt. %

Geol. an. Balk. poluos., 2023, 84 (1), 47–63

59

two elements. Likewise, melts with fractional magnetite crystallization show depleted concentrations of Ni and Co in the remaining silicate melt. After the formation of immiscible sulfides, Cu and Au are transferred from the melt to the sulfides, and the ore-forming potential of the remaining melt becomes reduced (Richards, 2015).

All analyzed bulk rock samples from Bor, and Čukaru Peki imply that the source magma in these deposits underwent amphibole fractionation and sulfide saturation. This follows the general assumption that both deposits were formed in the same geodynamic conditions but also implies that they might originate from the same or similar magma chamber.

Constraints from the Geochronological data

Geochronology results indicate that the initial mineralization at Čukaru Peki (constrained by the age of P2 porphyry intrusive) occurred around 86.5 Ma (±1.3 Ma). The final termination of the mineralization- marked by the age of late non-mineralized P10 porphyries happened at around 85.03±1.28 Ma.

Zircons from Bor yield somewhat similar ages:

– Host rock andesites yield ages between 85.6–84.8Ma;

– Deep porphyry diorites from Borska Reka yield ages between 84.5–82 Ma;

– Post-mineral porphyries yield ages around 83.25 Ma.

Considering that deep porphyry diorites and post-mineral porphyries are related to mineralization, we can conclude that the mineralizing event at Bor happened in a period between 84.5 and 82 Ma. Although this implies that the Bor system is younger than Čukaru Peki, we should also consider that the analytical precision of the LA-ICP-MS method is between 1 and 3% (Chiaraida et al., 2013; von Quadt et al., 2014). If the maximum values of analytical uncertainties are considered, the obtained ages of Bor and Čukaru Peki overlap.

The obtained data set is per previous U-Pb measurements of zircons from the Timok magmatic complex, which have concluded that the main mineralization event in this magmatic complex

happened at around 86–84 Ma (von Quadt et al., 2002; Banješević, 2010; Kolb et al., 2013).

The occurrence of two or more relatively adjacent porphyry systems with similar ages is common in porphyry systems worldwide, as illustrated in numerous examples by Sillitoe (2010) and references therein. The same author argues that porphyry clusters reflect the intermittent activities of large magma chambers. Another explanation for the difference in magmatic ages in Timok magmatic complex is provided by Kolb et al. (2013). These authors argue that the slab rollback during the formation of this magmatic arc results in different ages of mineralized systems. This is further supported by the fact that the oldest magmatic rocks are in the eastern part of the complex (in present-day orientation) and that the age of rocks gradually decreases by moving to the western part.

Conclusions

We have performed bulk rock analyses and zircon geochronology measurements to obtain new data about rocks' age and geochemical affinity in two world-class porphyry systems in the Timok magmatic complex: Bor and Čukaru Peki.

The results of the bulk rock analysis imply that the magma chambers, which are responsible for the hydrothermal systems of Bor and Čukaru Peki, show a similar development. Both of them underwent two crucial processes for the formation of porphyry systems:

1) High-pressure amphibole fractionation producing magma with adakitic affinity

2) Sulfide saturation of magma, which can explain the abundance of sulfur-rich minerals in these hydrothermal systems (pyrite, covellite, chalcocite, native sulfur)

The presented geochronological data implies that the main mineralization stage in this magmatic complex, which comprises Bor and Čukaru Peki, occurred in the period of 87 to 82 Ma, which corresponds with the activity of the first magmatic phase of this complex. The obtained mineralization ages of Čukaru Peki are very similar (between 86.5 and 85 Ma), with the obtained U-Pb ages of Bor (84.5-

82 Ma). Still, the age differences are within the span of maximum analytical uncertainties.

Acknowledgements

References

Banješević, M. 2010. Upper Cretaceous magmatic suites of the Timok magmatic complex. *Geološki anali Balkanskoga poluostrva*, 71: 13–22.

Banješević, M. & Large, D. 2014. Geology and mineralization of the new copper and gold discovery south of Bor Timok magmatic complex. *Proceedings of the XVI Serbian Geological Congress, Serbian Geological Society, Donji Milanovac, 2014*, 739–741.

Banješević, M., Cvetković, V., von Quadt, A., Ljubović-Obradović, D., Vasić, N., Pačevski, A. & Peytcheva, I. 2019. New Constraints on the Main Mineralization Event Inferred from the Latest Discoveries in the Bor Metallogenetic Zone (BMZ, East Serbia). *Minerals*, 9 (11): 672.

Bokhari, S.N.H., & Meisel, T.C. 2017. Method development and optimisation of sodium peroxide sintering for geological samples. *Geostandards and Geoanalytical Research*, 41 (2): 181–195.

Castillo, P.R. 2012. Adakite petrogenesis. *Lithos*, 134: 304–316.

Chiaradia, M., Schaltegger, U., Spikings, R., Wotzlaw, J. F. & Ovtcharova, M. 2013. How accurately can we date the duration of magmatic-hydrothermal events in porphyry systems?—an invited paper. *Economic Geology*, 108 (4): 565–584.

Clark, A.H. & Ullrich, T.D. 2004. ^{40}Ar-^{39}Ar age data for andesitic magmatism and hydrothermal activity in the Timok Massif, eastern Serbia: implications for metallogenetic relationships in the Bor copper-gold subprovince. *Mineralium Deposita*, 39 (2): 256–262.

Davidson, J., Turner S., Handley H., Macpherson C. & Dosseto, A. 2007. Amphibole "sponge" in arc crust? *Geology*, 35 (9): 787–790.

Defant, M.J. & Drummond, M.S. 1990. Derivation of some modern arc magmas by melting of young subducted lithosphere. *Nature*, 347: 662–665.

Đorđević, M. 2005. Volcanogenic Turonian and epiclastics of senonian in the Timok magmatic complex between Bor and the Tupižnica mountain, eastern Serbia. *Geoloski anali Balkanskoga poluostrva*, 66: 63–71.

Fügenschuh, B. & Schmid, S. M. 2005. Age and significance of core complex formation in a very curved orogen: Evidence from fission track studies in the South Carpathians (Romania). *Tectonophysics*, 404 (1–2): 33–53.

Gallhofer, D., Quadt, A. V., Peytcheva, I., Schmid, S. M. & Heinrich, C. A. 2015. Tectonic, magmatic, and metallogenic evolution of the Late Cretaceous arc in the Carpathian-Balkan orogen. *Tectonics*, 34 (9): 1813–1836.

Guillong, M., Meier, D.L., Allan, M.M., Heinrich, C.A. & Yardley, B.W. 2008. Appendix A6: SILLS: A MATLAB-based program for the reduction of laser ablation ICP-MS data of homogeneous materials and inclusions. In: Sylvester, P. (Ed.). *Laser Ablation ICP-MS in the Earth Sciences: Current Practices and Outstanding Issues*. Mineralogical Association of Canada Short Course Series, 40: 328–333.

Günther, D., Quadt, A.V., Wirz, R., Cousin, H. & Dietrich, V.J. 2001. Elemental analyses using laser ablation-inductively coupled plasma-mass spectrometry (LA-ICP-MS) of geological samples fused with Li2B4O7 and calibrated without matrix-matched standards. Microchimica Acta 136:101–107

Halley, S. 2020. Mapping Magmatic and Hydrothermal Processes from Routine Exploration Geochemical Analyses. *Economic Geology*, 115 (3): 489–503.

Jackson, S.E., Pearson, N.J., Griffin, W.L. & Belousova, E.A. 2004. The application of laser ablation-inductively coupled plasma-mass spectrometry to in situ U–Pb zircon geochronology. *Chemical Geology,* 211: 47–69.

Jakubec, J., MacSporran, G., Duinker, P., Pittuck, M., Manoljović, P., Sucharda, M., Samouković, M., Bunyard, C. & Arseneau, G. 2018. NI 43-101 *Technical Report-Timok Copper-Gold Project, Serbia: Upper Zone Prefea-*

Geol. an. Balk. poluos., 2023, 84 (1), 47–63

61

sibility Study and Resource Estimate for the Lower Zone, Nevsun Resources Ltd, 1–427.

Janković, S., Jovanović, M., Karamata, S. & Lovrić, A. 1981. Isotopic Age of Some Rocks from the Timok Eruptive Area (in Serbian). *Academy of Serbian Science and Arts, Natural Science and Mathematics*, 48: 87–94.

Janković, S. 1990. *The ore deposits of Serbia: Regional metallogenic settings, environments of deposition, and types.* Faculty of Mining and Geology, Belgrade (in Serbian with English summary).

Janković, S., Jelenković, R. & Koželj, D. 2002. *The Bor copper and gold deposit.* QWERTY, Bor

Jelenković, R., Koželj, D. & Serafimovski, T. 2001. Some genetic aspects of the Bor copper-gold deposit (Serbia). *Geologica Macedonica,* 15: 1–5.

Jelenković, R. 2014. A brief overview of the metallic mineral resources of Serbia. *European Geologist,* 37: 34–38.

Jelenković, R., Milovanović, D., Koželj, D. & Banješević, M. 2016. The mineral resources of the Bor metallogenic zone: a review. *Geologia Croatica*, 69 (1): 143–155.

Kennedy, A.K., Wotzlaw, J.F., Schaltegger, U., Crowley, J.L. & Schmitz, M. 2014. Eocene zircon reference material for microanalysis of U-Th-Pb isotopes and trace elements. *Canadian Mineralogist*, 52: 409–421.

Klimentyeva, D., Driesner, T., von Quadt, A., Tončić, T. & Heinrich, C. 2021. Silicate-replacive high sulfidation massive sulfide orebodies in a porphyry Cu-Au system: Bor, Serbia. *Mineralium Deposita*, 56: 1423–1448.

Klimentyeva, D. 2022. *Porphyry Cu – epithermal – massive sulfide ore system of Bor (Serbia):*

mass balance and geochronological perspective, PhD thesis, ETH Zurich, 161 pp.

Klimentyeva, D., Velojic, M., Von Quadt, A. & Hood, S. 2022. Interpretation of Trace Element Chemistry of Zircons from Bor and Cukaru Peki: Conventional Approach and Random Forest Classification. *Geosciences*, 12 (11): 396.

Knaak, M., Márton, I., Tosdal, R.M., Van der Toorn, J., Davidović, D., Strmbanović, I. & Hasson, S. 2016. Geologic setting and tectonic evolution of porphyry Cu-Au, polymetallic replacement, and sedimentary rock-hosted Au deposits in the northwestern area of the Timok magmatic complex, Serbia. Serbia: *Society of Economic Geologists, Special Publication*, 19: 1–28.

Kolb, M., von Quadt, A., Peytcheva, I., Heinrich, C.A., Fowler, S.J. & Cvetković, V. 2013. Adakite-like and normal arc magmas: distinct fractionation paths in the East Serbian segment of the Balkan–Carpathian arc. *Journal of Petrology*, 54 (3): 421–451.

Lerouge, C., Bailly, L., Béchu, E., Fléhoc, C., Genna, A., Lescuyer, J.L., Stein, G., Gillot, P.Y. & Kozelj, D. 2005. Age and origin of advanced argillic alteration at the Bor Cu-Au deposit, Serbia. *Mineral Deposit Research: Meeting the Global Challenge*, 541–544.

Ling, M.X., Liu, Y., Zhang, H. & Sun, W. 2014. Sample preparation and X-ray fluorescence analysis of sulfide ores. *Analytical Letters*, 47: 1598–1605.

Lips, A.L., Herrington, R.J., Stein, G., Kozelj, D., Popov, K. & Wijbrans, J.R. 2004. Refined timing of porphyry copper formation in the Serbian and Bulgarian portions of the Cretaceous Carpatho-Balkan Belt. *Economic Geology*, 99 (3): 601–609.

Menant, A., Jolivet, L., Tuduri, J., Loiselet, C., Bertrand, G. & Guillou-Frottier, L. 2018. 3D subduction dynamics: A first-order parameter of the transition from copper- to gold-rich deposits in the eastern Mediterranean region. *Ore Geology Reviews*, 94: 118–135.

Neubauer, F. 2002. Contrasting Late Cretaceous with Neogene ore provinces in the Alpine-Balkan-Carpathian-Dinaride collision belt: *Geological Society London Special Publication*, 204: 90–100.

Paton, C., Hellstrom, J., Paul, B., Woodhead, J. & Hergt, J. 2011. Iolite: Freeware for the visualisation and processing of mass spectrometric data. *Journal of Analytical Atomic Spectrometry*, 26: 2508–2518.

Richards, J.P. 2005. Cumulative factors in the generation of giant calc-alkaline porphyry Cu deposits. *Super porphyry copper and gold deposits: A global perspective*, 1: 7–25.

Sillitoe, R.H. 2010. Porphyry copper systems. *Economic geology*, 105 (1): 3–41.

Sláma, J., Košler, J., Condon, D.J., Crowley, J.L., Gerdes, A., Hanchar, J.M., Horstwood, M.S., Morris, G.A., Nasdala, L., Norberg, N. & Schaltegger, U. 2008. Plešovice zircon – A new natural reference material for U–Pb and Hf isotopic microanalysis. *Chemical geology* 249 (1-2): 1–35.

Starostin, V. 1970. Bor and Maidanpek copper deposits in Yugoslavia. *International Geology Review* 12: 370–380.

Stein, G., Koželj, D., Lips, A. & Bailly, L. 2002. The Timok Magmatic Complex (Serbia); An Adakitic Related Magmatic Event. *Geology and Metallogeny of Copper and Gold Deposits in the Bor Metallogenic Zone Bor 100*

62

Geol. an. Balk. poluos., 2023, 84 (1), 47–63

Years International Symposium, Bor Lake, Yugoslavia, 133–137.

Sun, S.S. & McDonough, W.F. 1989. Chemical and isotopic systematics of oceanic basalts: implications for mantle composition and processes. *Geological Society, London, Special Publications*, 42 (1): 313–345.

Vermeesch, P. 2018. IsoplotR: A free and open toolbox for geochronology. *Geoscience Frontiers,* 9: 1479–1493

von Quadt, A. Peytcheva, I., Cvetković, V., Banješević, M. & Koželj, D. 2002. Geochronology, geochemistry and isotope tracing of the Cretaceous magmatism of East-Serbia as part of the Apuseni-Timok-Srednogorie metallogenic belt. *Geologica Carpathica*, 53: 175–177.

von Quadt, A., Peytcheva, I., Heinrich, C., Cvetković, V., Banjesević, M. & Andrew, C.J. 2007. Upper Cretaceous magmatic evolution and related Cu–Au mineralization in Bulgaria and Serbia. *9th Biennial Meeting of the Society for Geology Applied to Mineral Deposits SGA, Dublin. Dublin: Irish Association for Economic Geology,* 861–864.

von Quadt, A., Gallhofer, D., Guillong, M., Peytcheva, I., Waelle, M. & Sakata, S. 2014. U–Pb dating of CA/non-CA treated zircons obtained by LA-ICP-MS and CA-TIMS techniques: impact for their geological interpretation. *Journal of Analytical Atomic Spectrometry*, 29 (9): 1618–1629.

Wiedenbeck, M., Alle, P., Corfu, F., Griffin, W.L., Meier, M., Oberli, F.V., Quadt, A.V., Roddick, J.C. & Spiegel, W. 1995. Three natural zircon standards for U-Th-Pb, Lu-Hf, trace element and REE analyses. *Geostandards newsletter,* 19 (1): 1–23.

Zimmerman, A., Stein, H.J., Hannah, J.L., Koželj, D., Bogdanov, K. & Berza, T. 2008. Tectonic configuration of the Apuseni–Banat—Timok–Srednogorie belt, Balkans-South Carpathians, constrained by high precision Re–Os molybdenite ages. *Mineralium Deposita*, 43 (1): 1–21.

Резиме

Нови подаци о геохемијском афинитету и старости минерализованих стена у Тимочком магматском комплексу, источна Србија

У овом раду су приказани нови резултати анализа геохемијских афинитета стена и старости циркона из два велика порфирска лежипта у Тимочком магматском комплексу: Бор и Чукару Пеки.

Добијени резултати анализа целих стена указују да су хидротермални системи Бор и Чукару формирани из магматских интрузива који су имали сличан развој. Оба магматска интрузива имају адакитски карактер и указују да се током њиховог развоја десила два важна процеса: фракционација амфибола и засићење судфидима.

Нови геохронолошки подаци указују да се главна фаза минерализације у Тимочком магматском комплексу, током које су формирани Бор и Чукару Пеки, десила у периоду између 87 до 82 Ma. Добијене старости се поклапају са активношћу прве вулканске фазе Тимочког магматског комплекса. Измерене старости минерализације система Чукару Пеки (86,5–85 Ma) се донекле разликују од добијених старости за Борски систем (84,5–82 Ma). Међутим добијене вредности се поклапају ако се урачунају максималне вредности аналитичке грешке за коришћену методу (око 1 до 2 Ma).

Geol. an. Balk. poluos., 2023, 84 (1), 47–63

63